COMBINED HF-ND-SR ISOTOPIC CONSTRAINTS ON THE MINERALOGICAL CHARACTERISTICS OF MARE BASALT SOURCES.

Amy M. Gaffney, Lars E. Borg, and Ross W. Williams, Lawrence Livermore National Laboratory, 7000 East Ave. L-235. Livermore, CA 94550; (gaffney1@llnl.gov).

Introduction: Crystallization of the lunar magma ocean during the earliest stages of the Moon's history is thought to have resulted in chemical differentiation of the Moon. Subsequent lunar magmatism tapped sources in the lunar interior and therefore provides a means with which to investigate the compositional diversity of the magma ocean crystallization products. The chemical and mineralogical variability of magma sources is reflected in the wide compositional range of magmas that originate from these sources. Thus, lunar basalts provide an important geochemical basis for the magma ocean model. Different parent-daughter element pairs are primarily fractionated by different minerals; for example the Lu/Hf ratio is controlled by ilmenite and garnet, the Rb/Sr ratio is controlled by plagioclase, and the Sm/Nd ratio is controlled by clinopyroxene. Therefore, the long-term ^{176}Lu/^{177}Hf-^{147}Sm/^{144}Nd-^{87}Rb/^{86}Sr compositions of lunar basalt sources, as determined from their Hf, Nd and Sr isotopic compositions, provide a valuable geochemical tool for constraining the mineralogical characteristics of the basalt sources.
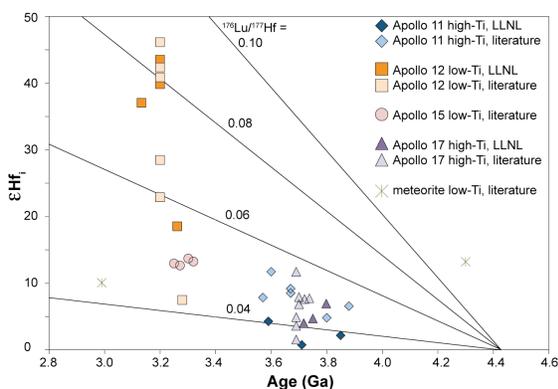

Figure 1. Age vs. initial Hf isotopic variation of lunar basalts reflects the variation in ^{176}Lu/^{177}Hf composition of the sources from which the basalts were derived. Diagonal lines reflect the Hf isotopic evolution of sources with different ^{176}Lu/^{177}Hf ratios, as labeled in the diagram, assuming differentiation of a chondritic Moon at 4.42 Ga. εHf notation indicates deviation of the sample ^{176}Hf/^{177}Hf from the chondritic value, in parts per 10^4. Literature data are from [2-5].

Analytical Techniques: A suite of 25 mare basalts, encompassing the range of petrogenetic types represented in the lunar sample collection, has been selected for whole rock Lu-Hf, Sm-Nd and Rb-Sr isotopic analysis. Analyses of 10 of these samples are complete, and analyses of the remainder are underway. Approximately 100 mg of each sample are digested in HF+HNO$_3$, using a Parr pressure digestion vessel. Af-

ter pressure digestion, samples are brought into a clear solution using first aqua regia then 6N HCl. Samples are then aliquoted for analysis of different isotope systems and spiked accordingly with mixed ^{176}Lu-^{180}Hf, ^{87}Rb-^{84}Sr and ^{149}Sm-^{150}Nd tracers. Hafnium is purified using first cation resin followed by DGA resin (Eichrom Industries). After separation of the REEs from the bulk sample using cation resin, Lu is purified using a 0.1 M α-HIBA column. Lu and Hf are analyzed on the Nu Plasma MC-ICP-MS. Rb, Sr, Sm and Nd are purified using our standard techniques [1] and analyzed on the ThermoElectron Triton TIMS.

Results and Discussion: The initial isotopic compositions of basalts reflect the long-term chemical history of the mantle sources of the basalts. Specifically, the initial isotopic composition of basalts are used to calculate the time-integrated parent-daughter ratios of the basalt source regions. This is demonstrated in the diagram of age vs. initial isotopic composition in Figure 1. The diagonal lines represent the Hf isotopic evolution of mantle sources of the basalts with ^{176}Lu/^{177}Hf ratios as given on the individual evolution lines. This model assumes chondritic evolution of the Moon until 4.42 Ga, at which time differentiation occurs and the mantle sources of the basalts are formed. This compositional information, in turn, is used to constrain the mineralogical characteristics of the basalt sources and how they may have formed in the context of the magma ocean model. Variation of calculated ^{176}Lu/^{177}Hf vs. ^{147}Sm/^{144}Nd source compositions for the
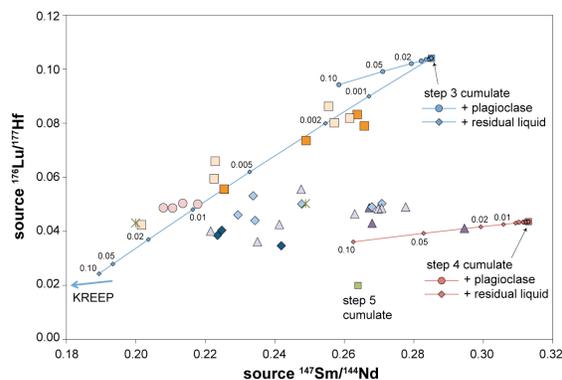

Figure 2. ^{176}Lu/^{177}Hf vs. ^{147}Sm/^{144}Nd variation of basalt sources. Modeled compositions of magma ocean cumulates follow models of Snyder et al. [6, 7]. Plotted cumulate step 3 and 4 compositions are plagioclase-free, with mixing lines showing the addition of small amounts of plagioclase and residual liquid (remaining after 95% crystallization). Numbers along mixing lines indicate fraction of plagioclase or residual liquid. Step 5 cumulate composition includes all the plagioclase that crystallized in this interval. Sample symbol legend and data sources in Fig. 1.

basalts requires two distinct sources at the depleted (high-^{147}Sm/^{144}Nd) end of the arrays.

Snyder et al. [6, 7] used the major element, trace element and Sr-Nd isotopic variation of mare basalts to construct a petrogenetic model for the formation of mare basalt sources during magma ocean crystallization, in which they determined that a combination of mafic cumulates ± plagioclase ± late-stage trapped liquid with the compositional characteristics of KREEP is required to account completely for chemical variation among the mare basalt sources. In order to understand the Lu/Hf variation of basalt sources in the context of lunar magma ocean crystallization, the results of the Snyder model, expanded to include Lu and Hf are presented in Figures 2 and 3. The model uses an updated set of partition coefficients for Lu, Hf, Sm and Nd [compiled in 8]. Modeled cumulate compositions for crystallization stages 3, 4 and 5 are shown. These crystallization stages represent 78-86%, 86-95%, and 95-99.5% crystallization, with modes of 25% ol + 53% plag + 22% pig, 36% plag + 26% pig + 38% cpx, and 31% plag + 34% pig + 24% cpx + 11% ilm, respectively [6].

For both ^{176}Lu/^{177}Hf vs. ^{147}Sm/^{144}Nd and ^{176}Lu/^{177}Hf vs. ^{87}Rb/^{86}Sr, the compositions of the low-Ti basalt sources are consistent with the derivation of these basalts from crystallization stage 3 cumulates + plagioclase (< 5%) + trapped liquid (< 2%). The compositions of the high-Ti basalt sources are consistent with the origin of the source endmember as a mixture between crystallization stage 5 cumulates and crystallization stage 4 cumulates ± plagioclase. These modeled compositions do not require the formation of garnet during magma ocean crystallization.

One important question in the petrogenesis of lunar basalts is: what is the role of ilmenite in the origin of the high-Ti basalts? Petrologic and geochemical arguments have been made both for ilmenite in the source
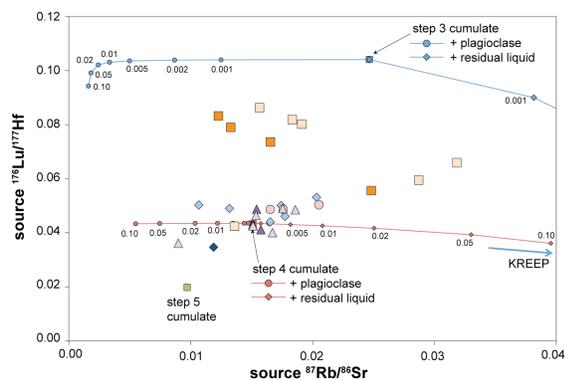
of the basalts [e.g., 9] and assimilation of ilmenite by magmas generated from an ilmenite-free source [e.g., 10]. Whether in the source or as an assimilant, ilmenite will have a strong influence on the Hf isotopic composition of the basalt. Ilmenite will have high Hf concentrations and unradiogenic ^{176}Hf/^{177}Hf, reflecting low time-integrated Lu/Hf. Ilmenite contribution to a basalt will effectively buffer the Hf isotopic composition of that magma. In Fig 2., assimilation of ilmenite by a low-Ti magma would drive points down, to lower ^{176}Lu/^{177}Hf (as represented by step 5 cumulates) at constant ^{147}Sm/^{144}Nd. In this scenario, it is expected that the compiled data would reflect the progression of assimilation, with a continuum of compositions between the low-Ti array and the high-Ti array. However, the compositional gap between low source ^{176}Lu/^{177}Hf and high source ^{176}Lu/^{177}Hf ratios at the high source ^{147}Sm/^{144}Nd end of the spectrum is not consistent with this expectation. Likewise, basalt TiO$_2$ content is not correlated with source ^{176}Lu/^{177}Hf variation in the high-Ti basalts. However, correlation of these two parameters is expected in the case of ilmenite assimilation (Fig. 4). Although our results can not definitively rule out the possibility of ilmenite assimilation, these geochemical relationships argue against this process as the controlling factor for the Hf isotopic composition of the high-Ti basalts.
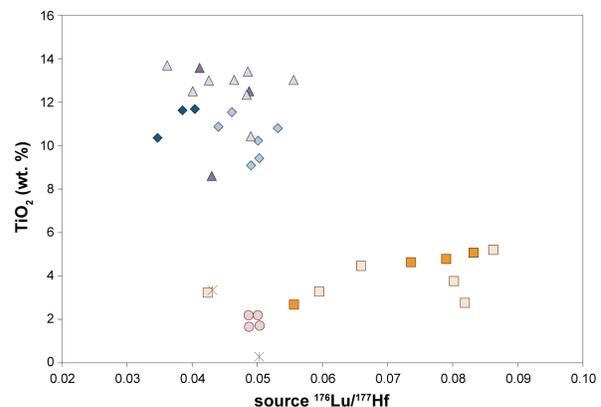

Figure 4. TiO$_2$ vs. source ^{176}Lu/^{177}Hf variation of basalts. Lu-Hf data sources in Fig. 1; TiO$_2$ data from author's compilation of literature data, references available upon request.

References: [1] Borg L. E. (2005) *GCA* 69:5819-5830; [2] Unruh D. M. et al.(1984) *JGR Suppl* 89:459-477; [3] Beard B. L. et al. (1998) *GCA* 62:525-544; [4] Sokol A. K. et al.(2008) *GCA* 72:4845-4873; [5] Brandon, A. D. et al. (2009) *GCA* 73:6421-6445; [6] Snyder G. A. et al. (1992) *GCA* 56:3809-3823; [7] Snyder G. A. et al. (1997) *GCA* 61:2731-2747; [8] Munker, C. (2010) *GCA* 74:7340-7361; [9] Ringwood A. E. and Kesson S. E. (1976) *LPSC* 1697-1722; [10] Hubbard N. J. and Minear J. W. (1975) *LPSC* 1057-1085.

Figure 3. ^{176}Lu/^{177}Hf vs. ^{147}Sm/^{144}Nd variation of basalt sources. See Fig. 1 and Fig. 2 for model detail and symbol legend and Lu-Hf data sources. Rb-Sr data from author's compilation of literature data, references available upon request.